UC Davis
UC Davis Previously Published Works

Title

Acute bone loss following SARS-CoV-2 infection in mice.

Permalink

https://escholarship.org/uc/item/5f38v74w

Journal

Journal of Orthopaedic Research, 41(9)

Authors

Haudenschild, Anne

Christiansen, Blaine

Orr, Sophie

et al.

Publication Date

2023-09-01

DOI

10.1002/jor.25537

Peer reviewed

Acute Bone Loss Following SARS-CoV-2 Infection in Mice

Anne K. Haudenschild[1], **Blaine A. Christiansen**[1], **Sophie Orr**[1], **Erin E. Ball**[2], **Christopher M. Weiss**[3], **Hongwei Liu**[3], **David P. Fyhrie**[1], **Jasper H.N. Yik**[1], **Lark L. Coffey**[2], **Dominik R. Haudenschild**[1]

[1]Department of Orthopaedic Surgery, University of California Davis Health, Sacramento, CA, 95817 USA 94065 USA

[2]Department of Pathology, Microbiology, and Immunology, University of California Davis School of Veterinary Medicine, Davis, CA 95616 USA

[3]Meissa Vaccines, Redwood City, CA 95817 USA

Abstract

The novel coronavirus disease 2019 (COVID-19) is caused by severe acute respiratory syndrome coronavirus 2 (SARS- CoV-2) and has infected more than 650 million people worldwide. Approximately 23% of these patients developed lasting "long-haul" COVID symptoms, including fatigue, joint pain, and systemic hyperinflammation. However, the direct clinical impact of SARS-CoV-2 infection on the skeletal system including bone and joint health has not been deter- mined. Utilizing a humanized mouse model of COVID-19, this study provides the first direct evidence that SARS-CoV- 2 infection leads to acute bone loss, increased osteoclast number, and thinner growth plates. This bone loss could decrease whole-bone mechanical strength and increase the risk of fragility fractures, particularly in older patients, while thinner growth plates may create growth disturbances in younger patients. Evaluating skeletal health in patients that have recovered from COVID-19 will be crucial to identify at-risk populations and develop effective countermeasures.

Graphical Abstract

SARS-CoV-2 infection leads to acute bone loss, and increased osteoclast number. This bone loss could decrease whole-bone mechanical strength and increase the risk of fractures. Evaluating skeletal health in patients that have recovered from COVID-19 will therefore be crucial for diagnosing and treating those at increased risk of fragility fractures and growth abnormalities.
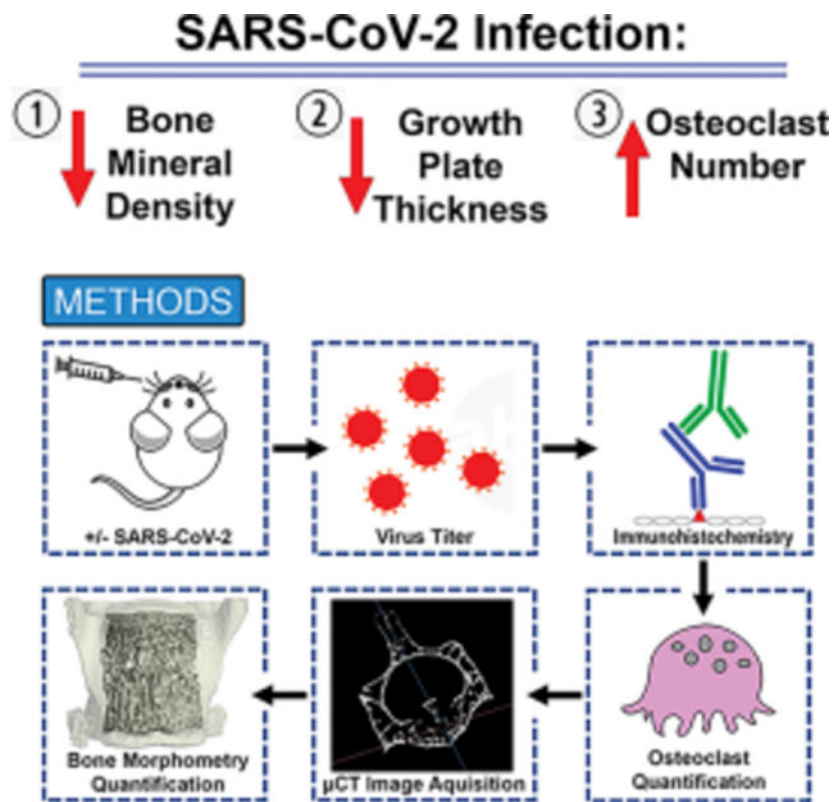
1 | INTRODUCTION

As of January 2023, the novel coronavirus disease 2019 (COVID-19) has infected more than 650 million people and killed over 6.7 million people worldwide [1]. COVID-19 is caused by severe acute respiratory syndrome coronavirus 2 (SARS-CoV-2), a coronavirus that binds to angiotensin-converting enzyme 2 (ACE2) receptors on cells [2]. SARS-CoV-2 infection can cause severe acute respiratory syndrome (SARS) and in severe cases can lead to systemic hyperinflammation and long-term damage to multiple organs.

Many patients fully recover from COVID-19 within a few weeks, but some continue to exhibit symptoms for four weeks or more after diagnosis [3]. In a study of approximately 2 million people diagnosed with COVID-19 in 2020 (including mild and asymptomatic cases), 23% reported having one or more health issues at least 30 days after diagnosis. The most common symptoms included chronic pain, trouble breathing, high cholesterol, fatigue, and high blood pressure [4]. Another study of long-COVID patients (those with symptoms ranging from 14 to 110 days post- infection) reported that approximately 80% of these infected patients developed one or more long-term symptoms, including fatigue (58%), difficult or labored breathing (24%), and joint pain (19%) [5].

Musculoskeletal tissues may also be affected by SARS-CoV-2 infection [6], and long-term symptoms may increase the risk of osteoporotic fractures or accelerate the progression of osteoarthritis. Musculoskeletal symptoms such as fatigue, muscle pain, and joint pain are common in patients with COVID-19 [6]. Systemic inflammation associated with COVID-19 may contribute to bone and joint pathology, and COVID-19 induced hypoxia can further increase the production of inflammatory cytokines. SARS-CoV-2 infection has been shown to trigger a hyperinflammatory state characterized by elevation of specific inflammatory markers, including lymphocyte count, neutrophil count, and C-reactive protein (CRP) [7, 8]. Additionally, COVID patients treated with corticosteroids could experience significant bone loss during treatment [9], and long-term bed rest and decreased physical ability could lead to disuse-induced bone loss. Altogether, these findings suggest that bone loss may be a serious comorbidity associated with COVID-19 that could lead to an increased incidence of fractures. However, the effect of SARS-CoV-2 infection on musculoskeletal tissues has not yet been examined.

2 | METHODS AND MATERIALS

2.1 | Ethics statement

Mouse work was conducted under protocol #21868 approved by the institutional animal care and use committee (IACUC) at the University of California, Davis. Infectious virus was handled in certified animal biosafety level 3 laboratory (ABSL-3) spaces in compliance with approved biological use authorization #R2813. The University of California, Davis, is accredited by the Association for Assessment and Accreditation of Laboratory Animal Care (AAALAC). All mouse work adhered to the NIH Guide for the Care and Use of Laboratory Animals.

2.2 | Mice

Equal numbers of male and female transgenic mice expressing the human ACE2 receptor on a K18 transgene in a C57Bl/6J background (B6.Cg.Tg(K18-ACE2)2Prlmn/J, 'hACE2') were purchased at five weeks of age from Jackson Laboratories (Sacramento, CA). Mice were co-housed by sex in ABSL-3 conditions with four animals per cage and acclimated for up to six days at 22–25 °C and a 12:12 hour light: dark cycle. Rodent chow with 18% protein content and sterile bottled water was provided *ad libitum*.

2.3 | Virus

SARS-CoV-2/human/USA/CA-CZB-59X002/2020 (GenBank #MT394528), which was isolated from a patient in 2020 in Northern California and passaged once in Vero-E6 cells, was provided by Dr. Christopher Miller (University of California, Davis). To generate stocks for this study, SARS-CoV-2 was passaged one additional time in Vero-E6 cells. Single-use virus aliquots were stored at −80 °C until used in mouse studies.

2.4 | SARS-CoV-2 challenge of mice

Six-week-old mice were inoculated with 103 or 104 plaque-forming units (PFU) of a 2020 SARS-CoV-2 strain (GenBank Accession number MT394531) (12 male, 12 female) or mock-inoculated with phosphate-buffered saline (Control) (4 male, 4 female). Inoculations

were performed via the intranasal (i.n.) route using a hanging drop applied into the nose under isoflurane anesthesia. Inocula were back-titrated to confirm the target dose. Mice were monitored twice daily for changes in weight, ruffled fur, ataxia, and labored breathing for up to 14 days. On days 1–6, mice were anesthetized with isoflurane, and throats were swabbed with rayon-tipped swabs (Puritan, Fisher Scientific, Waltham, MA). Mice were euthanized prior to experimental endpoint if weight loss exceeded 20% of the starting weight or if animals were deemed moribund as evidenced by limb weakness, ataxia or dragging of limbs, loss of limb function, or rapid or depressed respiration rate. An adverse event was defined as any moribund disease signs at any time over the duration of the experiment. Mice were euthanized by isoflurane overdose and cervical dislocation, then perfused with cold, sterile PBS.

2.5 | Measurement of viral burden

Swabs were vortexed briefly in 400 μL of Dulbecco's Modified Eagles Medium (DMEM, Fisher Scientific, Waltham, MA) and frozen at -80 °C. The lung (right inferior lobe) and brain (left hemisphere) were weighed and homogenized in 1–10 μL/mg DMEM with a sterile glass bead at 30 Hz for 4 minutes using a TissueLyser (Qiagen, Germantown, MD) automated homogenizer. Homogenates were cleared by centrifugation at 10,000 x g for 4 minutes and the cleared fraction was stored at -80 °C. Titrations by plaque assay to measure infectious virus were determined from back titrations of inocula, throat swabs, and homogenates of lungs and brain using established protocols [10, 11].

2.6 | Assessment of bone microstructure in rodents using microCT

To determine systemic bone loss following SARS-CoV-2 infection, lumbar spines (SARS-CoV-2: n = 24 at 7 ± 2.2 days post-infection; Control: n = 8 at 14 days after mock-inoculation) were scanned with micro-computed tomography (SCANCO μCT 35, Brüttisellen, Switzerland) with X-ray tube potential = 55 kVp, intensity = 114 μA, 6 μm isotropic nominal voxel size, integration time = 900 ms. The fifth lumbar (L5) vertebra was identified, and manual contouring and segmentation were performed on the trabecular region of the L5 vertebral body by a single experienced operator (BAC). The microstructure of the trabecular bone region was processed using the standard protocol of SCANCO software for μCT analysis of trabecular bone. Based on the thresholded trabecular bone image, bone volume fraction (BV/TV) was determined by dividing the total bone voxel volume (BV) by the total volume (TV) of interest. Trabecular thickness (Tb.Th) was evaluated via a distance transformation of the 3-D bone image and then determined by the average diameter of the maximum spheres that fit inside the bone tissue. Trabecular number (Tb.N) was determined as the inverse of the mean distance between the midline of trabecular bone tissue. Bone surface density (BS/BV) was computed by dividing the trabecular bone surface (BS) by the trabecular bone volume (BV) [12].

2.7 | Immunohistochemistry

Mouse carcasses were extensively fixed in formalin to inactivate the SARS-CoV-2 virus. The L5 vertebrae, stifle joints, and lung were dissected, bones decalcified, and tissues processed for immunohistochemistry with antibodies to detect SARS-CoV-2 nucleoprotein (40143-T62 at 1:2000, Sino Bio), hACE2 (AF93 at 1:2000, R&D Systems), and TRAP

(PA5–116970 at 1:1000, ThermoFisher), using HRP-conjugated secondary antibodies, DAB substrate, and Meyer's Hematoxylin counterstain.

2.8 | Osteoclast Quantification

Osteoclast number per bone perimeter (Oc.N/B.Pm) was measured on the trabecular bone of the distal femoral epi- physis on sagittal images of the tibiofemoral joint TRAP immunohistochemistry slides (n = 10). Osteoclast count and trabecular bone perimeter length measurements were conducted using FIJI open-source image processing software [13] as previously described [14].

2.9 | Growth plate thickness measurements

Growth plate thickness was measured from sagittal images of the tibiofemoral joint of TRAP immunohistochemistry slides (n=30) at 3.5x magnification. A total of 10 thickness measurements per bone (femur and tibia) were collected per slide across the length of the growth plate using FIJI software [13] as previously described [15].

2.10 | Statistical analysis

All evaluations in this study were performed on data collected from SARS-CoV-2 infected mice (12 male, 12 female) and mock-inoculated (Control) mice (4 male, 4 female). Multivariable linear regression modeling was performed to determine the strength of the effect that multiple independent variables (sex, viral infection, and viral dose) had on each of the four dependent bone measurements (BV/TV, BS/BV, Tb.Th, and Tb.N) and five dependent viral measurements (throat swab titers at Day 1, Day 2, and Day 3, brain titers, and lung titers) using JMP Pro v16 (SAS Institute, Cary, NC). During the evaluation of bone microstructure, male and female data were analyzed separately to account for sex differences in bone structure ($p < 0.0002$ for all four bone measurements), and data from both viral doses were pooled because there was no significant effect of dose on bone measurements ($p > 0.42$ for all four bone measurements). For virologic outcomes, male and female mice were analyzed together because there was not a significant effect of sex on viral titers ($p > 0.40$ for all five viral measurements), and the 103 and 104 PFU viral dose data were analyzed separately to account for significant dose differences in viral measurements ($p < 0.02$ for all five virus measurements). The Log- rank (Mantel-Cox) test for survival proportions was performed pairwise, and p-values were adjusted with Bonferroni correction using the R version 4.0.0 (R Project) p.adjust function. Statistical analysis of bone-based measurements and neutralizing antibody data in SARS-CoV-2 vs. mock-inoculated groups was performed using a Student's t-test. Bar chart data are presented as the mean ± standard deviation with significant differences $(p<0.05)$ indicated by bars with an asterisk (*). Statistical analysis of virology data was performed using one-way ANOVA with Tukey's post-hoc analysis. Bar chart data are presented as the mean ± standard deviation with significant differences (p<0.05) indicated by bars not sharing the same letter.

2.11 | Data Availability

The data that support the findings of this study are available from the corresponding author upon reasonable request.

3 | RESULTS

In this study, we investigated acute bone loss following SARS-CoV-2 infection in 6-week-old transgenic mice expressing humanized ACE2 (hACE2) receptors (12 male, 12 female) compared to mock-inoculated (Control) mice (4 male, 4 female) (Fig. 1 A). Intranasal inoculation was selected to mimic human SARS-CoV-2 exposure, which occurs via the respiratory mucosa. SARS-CoV-2 infection at both 103 and 104 plaque-forming units (PFU) induced severe disease including weight loss, and mice were euthanized if they lost 20% of their starting weight (Fig. 1 B). SARS-CoV-2 infected mice lived for an average of 7 ± 2.2 days post-infection (Fig. 1 C) and showed a dose-response to lethal disease where all mice inoculated with 104 PFU met euthanasia criteria (n = 12), and 75% of mice inoculated with 103 PFU were euthanized (n = 9). Control mice did not exhibit weight loss and were euthanized at 14 days after mock-inoculation (n = 8). Infection was confirmed by enumerating virus in throat swabs (Fig. 1 D), lungs (Fig. 1 E), and brains (Fig. 1 F). All SARS-CoV-2 inoculated mice had detectable virus in at least one swab or tissue, and the surviving mice had neutralizing antibody at 14 days post-inoculation (Fig. 1 G). Infectious SARS-CoV-2 or antibody were not detected in samples from any mock-inoculated mice.

Immunohistochemical analysis demonstrated that the hACE2 receptor was expressed in multiple joint tissues, including bone marrow, synovial lining cells, adipose tissues, and chondrocytes (Fig. 2), suggesting that both bone and joint tissues are susceptible to viral infection in the hACE2 mouse COVID-19 model. We further assessed whether the SARS-CoV-2 coat protein nucleocapsid was detected in the joint tissues, which would indicate that the SARS-CoV-2 reached these tissues and infected the various cell types. We identified nucleocapsid-positive cells in the synovium, bone marrow, and cells in the distal femoral growth plate as well as in the lung (a positive control) (Fig. 2).

Clinically, COVID-19 in humans is associated with systemic inflammation in both children and adults [16]. To determine systemic bone loss following SARS-CoV-2 infection, lumbar spines were scanned with micro-computed tomography (microCT), and trabecular bone microstructure was analyzed in the fifth lumbar (L5) vertebral body (Fig. 3A). MicroCT analysis showed that SARS-CoV-2 infection was associated with significantly reduced trabecular bone volume fraction (BV/TV; −10 and −10.5%; *p= 0.04*), increased the specific bone surface (BS/BV; +12.7 and +14.4%; *p= 0.03*), reduced trabecular thickness (Tb.Th; −8.3 and −8.9%; *p= 0.02*), and increased trabecular number (Tb.N; +3.5 and +3.1% (*p< 0.05*) in male and female mice, respectively, compared to Control mice (Fig. 3B–E). These data are the first to show that SARS-CoV-2 infection can cause significant changes in bone microstructure, suggesting that decreased bone mass, increased fracture risk, and other musculoskeletal complications could potentially be long-term comorbidities for people with COVID-19.

To verify our microCT findings and gain mechanistic insight into the observed changes in trabecular bone architecture, osteoclast number was quantified using Tartrate-Resistant Acid Phosphatase type 5b (TRAP) immunohistochemistry at the distal femoral epiphysis (Fig. 4A). The TRAP enzyme regulates the activity of osteopontin, which is produced in osteoclasts and is considered a marker of bone resorption [17]. SARS-CoV-2 infection

significantly increased the number of osteoclasts on the trabecular bone perimeter (+37% (*p= 0.044*) (Fig. 4B). SARS-COV-2 infected mice also had significantly thinner growth plates in the distal femur (−40.3%; *p<0.0001*) and proximal tibia (−20.3%; *p=0.002*) as compared to Control mice (Fig. 4C). These data are the first confirmation of the deleterious effect of SARS-CoV-2 infection on bone resorption and growth plate thinning, suggesting that bone loss and growth disturbances may be serious complications in COVID-19 patients.

4 | DISCUSSION

In this study, we provide direct evidence that SARS-CoV-2 infection leads to acute bone loss, increased osteoclast number, and thinner growth plates. This bone loss could decrease whole-bone mechanical strength and increase the risk of fractures. Our previous studies on systemic bone loss in mice following femoral fracture found that recovery from such bone loss is diminished in older mice [14]. If a similar deficit in bone recovery occurs in human patients following recovery from COVID-19, this could leave older patients with a long-term or even permanent increased risk of osteoporotic fracture, which can lead to considerable morbidity and mortality [18]. Evaluating skeletal health in patients that have recovered from COVID-19 will therefore be crucial for diagnosing and treating those at increased risk of fragility fractures.

Clinically, 14.9% of all acute COVID-19 patients reported joint pain during viral infection including nonsevere (14.5%) and severe (17.3%) cases [29]. In addition, 35% to 90.5% of recovered patients who survive COVID-19 continue to have a wide variety of clinical manifestations [30], including joint pain (31.4%) [31] and reactive arthritis [32]. COVID-19 patients requiring intensive care had significantly lower BMD than those who were managed in non-intensive care settings [33]. COVID-19-induced inflammation has been found to negatively affect the musculoskeletal system through both direct and indirect mechanisms. SARS-CoV-2 enters cells by binding to the ACE2 receptor, a transmembrane protein important in angiotensin signaling that is also expressed in skeletal cells, including osteoblasts and osteoclasts [18]. It is well established in humans that ACE2 is found in the lung, heart, kidney, liver, gastrointestinal, and musculoskeletal systems [6]. More specifically, in the musculoskeletal system, proliferative, hypertrophic, and effector articular chondrocytes all express ACE2 and ACE2 is found in composite unenriched cortical and trabecular bone and osteoblast enriched tissues [6]. In skeletal cells, ACE2 has anti-inflammatory functions, restricts bone resorption, and promotes skeletal repair [20,21] which are the result of blocking the proinflammatory actions of angiotensin II [22]. When SARS-CoV-2 binds the ACE2 receptor, it may inhibit ACE2/angiotensin signaling, thus directly contributing to bone loss [19]. We established the presence of viral proteins in bone and joint tissues, suggesting that a direct effect of the virus may be observed in these tissues. In addition to these direct effects of SARS-CoV-2 on skeletal cells, indirect effects from systemic inflammation, hypoxia, and reduced mobility may also promote bone loss through increased production of inflammatory cytokines and activation of the nuclear factor-κB (RANK)/RANK ligand (RANKL) pathways that promote osteoclastogenesis [23, 24]. Given that a reduction in bone mass significantly increases the risk of bone fracture, it is important to continue to investigate the musculoskeletal effects and long-term bone health in COVID-19 patients. While previous studies have highlighted the adverse effects on

bone from chronic viral infections [25], it is critical to delineate the molecular mechanism of systemic bone loss induced by COVID-19 to identify at-risk populations and develop effective countermeasures.

Current data showing growth plate thinning following SARS-CoV-2 infection suggest that in younger patients, COVID-19 may affect skeletal growth and development. Growth arrest of long bone metaphyses has been reported in childhood diseases with a severe course of illness, malnourishment, infections, hypothyroidism, chronic juvenile arthritis, after the use of certain medications, and upon immobilization [26]. The direct cause of growth plate thinning in the present experiment is unknown; however, SARS-CoV-2 is reported to increase plasma Growth Arrest-Specific Factor 6 (GAS6) [27], which *in-vitro* can down-regulate chondrocyte proliferation [28]. Whether this is causal in our experiments was not tested.

The current study was somewhat limited by the use of juvenile (six-week-old) transgenic mice rather than adult or aged mice. This study administered lethal doses (10^3 or 10^4 plaque-forming units of SARS-CoV-2 virus) which caused infected mice to be euthanized approximately seven days post-infection and limited our analysis to a narrow window after acute infection. There were no significant differences between the 10^4 (high) and 10^3 (low) viral inoculations and resulting lung (*p = 0.95*) and brain (*p = 0.26*) titers or bone measurements (*p > 0.42* for all four bone measurements. For this reason, bone data from both viral doses were pooled. Clinically, 82.2% of severe COVID-19 cases and 53.9% of mild COVID-19 cases developed long COVID [34]. Additional studies at lower viral titer are necessary to examine longer timepoints of disease and whether the effects of mild infection produce similar bone loss. Additionally, the humanized mouse model expresses ACE2 in tissues and at levels where it may not be expressed in humans. We were not able to measure systemic inflammation, the activity level of mice, or other potential mechanisms driving acute bone loss. Despite these limitations, this study is the first to report that SARS-CoV-2 infection initiated a rapid loss of trabecular bone and decreased growth plate. We anticipate that this bone loss is likely driven by hyperinflammation and decreased mobility, together with the direct effects of the SARS-CoV-2 infection on bone cells. In humans, long and/or debilitating cases of COVID-19 may lead to profound and long-lasting bone loss; therefore, an as-of-yet unreported long-haul symptom of COVID-19 may be increased risk of fragility fractures. Recovery from this bone loss may take several months or even years or may be permanent in some cases. In addition, younger patients may also experience growth failure due to growth plate thinning and impaired longitudinal bone growth. Prospective clinical studies of COVID-19 patients should monitor these populations carefully for increased risk and incidence of fractures and growth abnormalities.

ACKNOWLEDGMENTS

references

[1]. World Health Organization. (2023, January 24). " WHO Coronavirus (COVID-19) Dashboard " Retrieved from https://covid19.who.int/

[2]. Huang C, Wang Y, Li X, Ren L, Zhao J, Hu Y, et al. Clinical features of patients infected with 2019 novel coronavirus in Wuhan, China. The Lancet 2020 Feb;395(10223):497–506. 10.1016/s0140-6736(20)30183-5.

[3]. Centers for Disease Control and Prevention, Post-COVID Conditions; 2021. https://www.cdc.gov/coronavirus/2019-ncov/long-term-effects/ [cited: 2021 November 19].

[4]. FAIR Health, Detailed Study of Patients with Long-Haul COVID, in An Analysis of Private Healthcare Claims [White Paper]; 2021. https://www.fairhealth.org/publications/whitepapers [cited: 2021 November 19].

[5]. Lopez-Leon S, Wegman-Ostrosky T, Perelman C, Sepulveda R, Rebolledo PA, Cuapio A, et al. More than 50 long-term effects of COVID-19: a systematic review and meta-analysis. Scientific Reports 2021 Aug;11(1). 10.1038/s41598-021-95565-8.

[6]. Disser NP, Micheli AJD, Schonk MM, Konnaris MA, Piacentini AN, Edon DL, et al. Musculoskeletal Consequences of COVID-19. Journal of Bone and Joint Surgery 2020 May;102(14):1197–1204. 10.2106/jbjs.20.00847.

[7]. Hu B, Huang S, Yin L. The cytokine storm and COVID-19. Journal of medical virology 2021;93(1):250–256. [PubMed: 32592501]

[8]. Nile SH, Nile A, Qiu J, Li L, Jia X, Kai G. COVID-19: Pathogenesis, cytokine storm and therapeutic potential of interferons. Cytokine & growth factor reviews 2020;53:66–70. [PubMed: 32418715]

[9]. Allen DB. Growth suppression by glucocorticoid therapy. Endocrinology and metabolism clinics of North America 1996;25(3):699–717. [PubMed: 8879994]

[10]. Mendoza EJ, Manguiat K, Wood H, Drebot M. Two Detailed Plaque Assay Protocols for the Quantification of Infectious SARS-CoV-2. Current Protocols in Microbiology 2020 May;57(1). 10.1002/cpmc.105.

[11]. Lakshmanappa YS, Elizaldi SR, Roh JW, Schmidt BA, Carroll TD, Weaver KD, et al. SARS-CoV-2 induces robust germinal center CD4 T follicular helper cell responses in rhesus macaques. Nature Communications 2021 Jan;12(1). 10.1038/s41467-020-20642-x.

[12]. Bouxsein ML, Boyd SK, Christiansen BA, Guldberg RE, Jepsen KJ, Müller R. Guidelines for assessment of bone mi- crostructure in rodents using micro-computed tomography. Journal of Bone and Mineral Research 2010 Jun;25(7):1468–1486. 10.1002/jbmr.141. [PubMed: 20533309]

[13]. Schindelin J, Arganda-Carreras I, Frise E, Kaynig V, Longair M, Pietzsch T, et al. Fiji: an open-source platform for biological- image analysis. Nature Methods 2012 Jun;9(7):676–682. 10.1038/nmeth.2019. [PubMed: 22743772]

[14]. Emami AJ, Toupadakis CA, Telek SM, Fyhrie DP, Yellowley CE, Christiansen BA. Age Dependence of Systemic Bone Loss and Recovery Following Femur Fracture in Mice. Journal of Bone and Mineral Research 2018 Sep;34(1):157–170. 10.1002/jbmr.3579. [PubMed: 30189111]

[15]. Lamuedra A, Gratal P, Calatrava L, Ruiz-Perez VL, Largo R, Herrero-Beaumont G. Disorganization of chondrocyte columns in the growth plate does not aggravate experimental osteoarthritis in mice. Scientific Reports 2020 Jul;10(1). 10.1038/s41598-020-67518-0.

[16]. Ramos-Casals M, Brito-Zerón P & Mariette X Systemic and organ-specific immune-related manifestations of COVID-19. Nat Rev Rheumatol 17, 315–332 (2021). 10.1038/s41584-021-00608-z [PubMed: 33903743]

[17]. Song L Calcium and Bone Metabolism Indices. In: Advances in Clinical Chemistry Elsevier; 2017.p. 1–46. 10.1016/bs.acc.2017.06.005.

[18]. Jiang HX, Majumdar SR, Dick DA, Moreau M, Raso J, Otto DD, et al. Development and Initial Validation of a Risk Score for Predicting In-Hospital and 1-Year Mortality in Patients With Hip Fractures. Journal of Bone and Mineral Research 2004 Nov;20(3):494–500. 10.1359/jbmr.041133. [PubMed: 15746995]

[19]. Queiroz-Junior CM, Santos ACPM, Galvão I, Souto GR, Mesquita RA, Sá MA, et al. The angiotensin converting enzyme 2/angiotensin-(1–7)/Mas Receptor axis as a key player in

alveolar bone remodeling. Bone 2019 Nov;128:115041. 10.1016/j.bone.2019.115041. [PubMed: 31442676]

[20]. Joshi S, Balasubramanian N, Vasam G, Jarajapu YP. Angiotensin converting enzyme versus angiotensin converting enzyme-2 selectivity of MLN-4760 and DX600 in human and murine bone marrow-derived cells. European Journal of Pharmacology 2016 Mar;774:25–33. 10.1016/j.ejphar.2016.01.007. [PubMed: 26851370]

[21]. Nozato S, Yamamoto K, Takeshita H, Nozato Y, Imaizumi Y, Fujimoto T, et al. Angiotensin 1–7 alleviates aging-associated muscle weakness and bone loss, but is not associated with accelerated aging in ACE2-knockout mice. Clinical Science 2019 Sep;133(18):2005–2018. 10.1042/cs20190573. [PubMed: 31519791]

[22]. Burrell LM, Johnston CI, Tikellis C, Cooper ME. ACE2, a new regulator of the renin–angiotensin system. Trends in Endocrinology & Metabolism 2004 May;15(4):166–169. 10.1016/j.tem.2004.03.001. [PubMed: 15109615]

[23]. Salvio G, Gianfelice C, Firmani F, Lunetti S, Balercia G, Giacchetti G. Bone Metabolism in SARS-CoV-2 Disease: Possible Osteoimmunology and Gender Implications. Clinical Reviews in Bone and Mineral Metabolism 2020 Sep;18(4):51–57. 10.1007/s12018-020-09274-3. [PubMed: 32904892]

[24]. Hardy R, Cooper MS. Bone loss in inflammatory disorders. Journal of Endocrinology 2009 Feb;201(3):309–320. 10.1677/joe-08-0568. [PubMed: 19443863]

[25]. Maltby S, Lochrin AJ, Bartlett B, Tay HL, Weaver J, Poulton IJ, et al. Osteoblasts Are Rapidly Ablated by Virus-Induced Systemic Inflammation following Lymphocytic Choriomeningitis Virus or Pneumonia Virus of Mice Infection in Mice. The Journal of Immunology 2017 Dec;200(2):632–642. 10.4049/jimmunol.1700927. [PubMed: 29212906]

[26]. Bilo R, Robben S, van Rijn R. Forensic Aspects of Paediatric Fractures; Differentiating Accidental Trauma from Child Abuse. Springer; 2010. Forensic Aspects of Paediatric Fractures; Differentiating Accidental Trauma from Child Abuse; Conference date: 01–01-2010.

[27]. Morales A, Rello SR, Cristóbal H, Fiz-López A, Arribas E, Marí M, et al. Growth Arrest-Specific Factor 6 (GAS6) Is Increased in COVID-19 Patients and Predicts Clinical Outcome. Biomedicines 2021 Mar;9(4):335. 10.3390/biomedicines9040335. [PubMed: 33810394]

[28]. Hutchison MR, Bassett MH, White PC. SCF, BDNF, and GAS6 Are Regulators of Growth Plate Chondrocyte Proliferation and Differentiation. Molecular Endocrinology 2010 Jan;24(1):193–203. 10.1210/me.2009-0228. [PubMed: 19897599]

[29]. Guan WJ, Ni ZY, Hu Y, Liang WH, Ou CQ, He JX, Liu L, Shan H, Lei CL, Hui DSC, Du B, Li LJ, Zeng G, Yuen KY, Chen RC, Tang CL, Wang T, Chen PY, Xiang J, Li SY, Wang JL, Liang ZJ, Peng YX, Wei L, Liu Y, Hu YH, Peng P, Wang JM, Liu JY, Chen Z, Li G, Zheng ZJ, Qiu SQ, Luo J, Ye CJ, Zhu SY, Zhong NS; China Medical Treatment Expert Group for Covid-19. Clinical Characteristics of Coronavirus Disease 2019 in China. N Engl J Med. 2020 Apr 30;382(18):1708–1720. doi: 10.1056/NEJMoa2002032. Epub 2020 Feb 28. [PubMed: 32109013]

[30]. Abdel-Gawad M, Zaghloul MS, Abd-Elsalam S, Hashem M, Lashen SA, Mahros AM, Mohammed AQ, Hassan AM, Bekhit AN, Mohammed W, Alboraie M. Post-COVID-19 Syndrome Clinical Manifestations: A Systematic Review. Antiinflamm Antiallergy Agents Med Chem. 2022

[31]. Fernández-de-Las-Peñas C, Palacios-Ceña D, Gómez-Mayordomo V, Florencio LL, Cuadrado ML, Plaza-Manzano G, Navarro-Santana M. Prevalence of post-COVID-19 symptoms in hospitalized and non-hospitalized COVID-19 survivors: A systematic review and meta-analysis. Eur J Intern Med. 2021;92:55–70. [PubMed: 34167876]

[32]. Sapkota HR, Nune A. Long COVID from rheumatology perspective - a narrative review. Clin Rheumatol. 2022;41:337–348. [PubMed: 34845562]

[33]. Kottlors J, Große Hokamp N, Fervers P, Bremm J, Fichter F, Persigehl T, Safarov O, Maintz D, Tritt S, Abdullayev N. Early extrapulmonary prognostic features in chest computed tomography in COVID-19 pneumonia: Bone mineral density is a relevant predictor for the clinical outcome - A multicenter feasibility study. Bone. 2021;144:115790. [PubMed: 33301962]
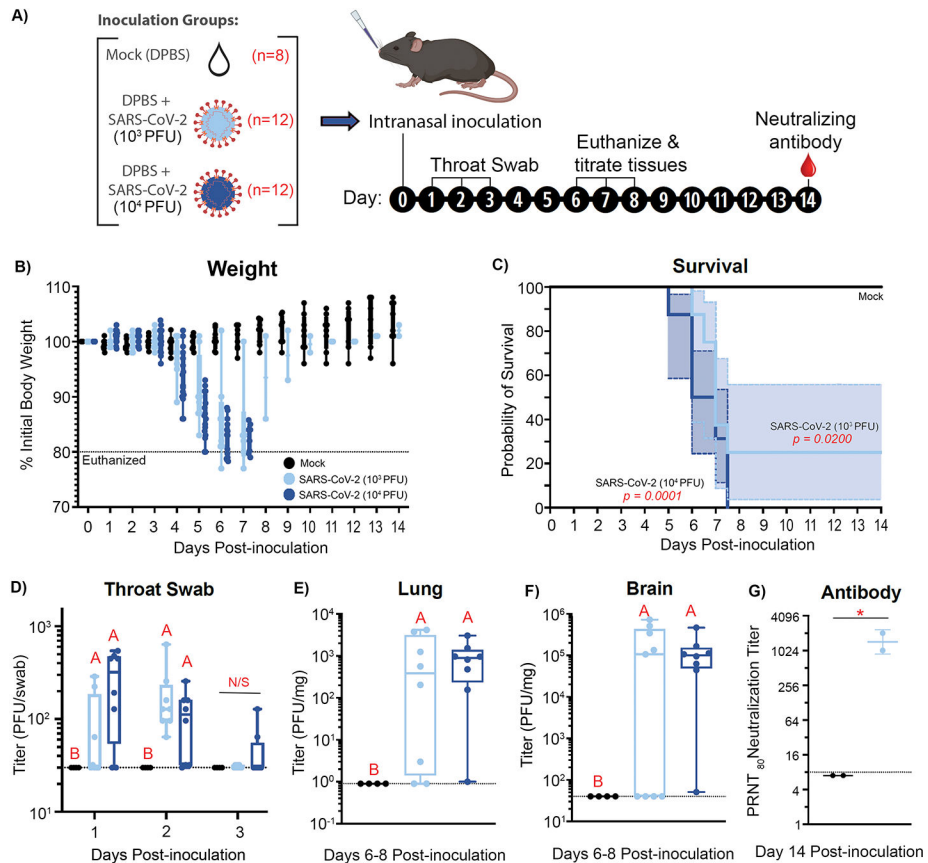
[34]. Cervia C, Zurbuchen Y, Taeschler P et al. Immunoglobulin signature predicts risk of post-acute COVID-19 syndrome. Nat Commun 13, 446 (2022). 10.1038/s41467-021-27797-1 [PubMed: 35078982]

Figure 1.
SARS-CoV-2 infection induced severe disease in mice. Intranasal administration of two doses of SARS-CoV- 2 to transgenic six-week-old male and female k18-hACE2 receptor-expressing mice (A) caused weight loss (B) and lethal disease (C). The p values on survival curves are comparing SARS-CoV-2 inoculated groups to mock-inoculated Control groups using a log-rank (Mantel-Cox) test for multiple comparisons with Bonferroni's correction. SARS-CoV- 2 was detected in throat swabs (D) and lung (E) and brain (F) collected at necropsy 6–8 days post-inoculation, and surviving mice developed neutralizingantibody (G). Neither SARS-CoV-2 nor neutralizing antibody was detected in any samples from mockinoculatedControl mice. Control mice were euthanized 14 days post-inoculation. Viral titers were measuredby plaque assay, and antibody was measured using plaque reduction neutralization 80 (PRNT80) as- says.Each measurement was conducted once. Significant differences (p<0.05) are indicated by bars with anasterisk (*) for comparison between two groups or bars not sharing the same letter for comparison betweenthree groups. No significant differences between groups are indicated by bars with a label of "N/S". Sampledata: SARS-CoV-2 (103 PFU) (6 male, 6 female), SARS-CoV-2 (104 PFU) (6 male, 6 female), or mockinoculatedwith phosphate-buffered saline (Control) (4 male, 4 female).
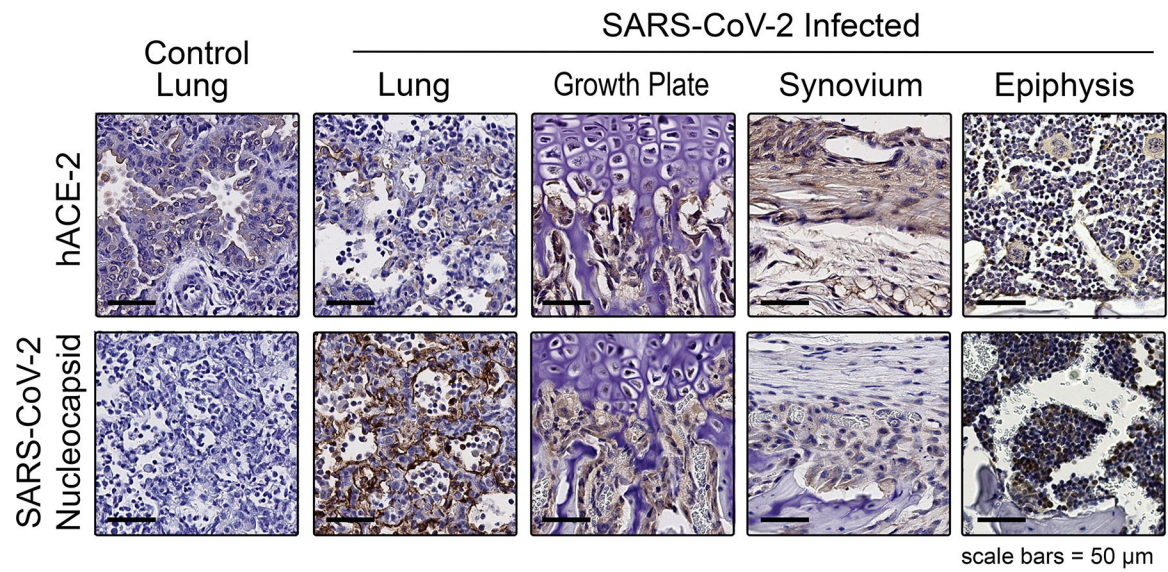
Figure 2.
Expression of hACE-2 receptor and SARS-CoV-2 positive cells in musculoskeletal tissues. ThehACE2 receptor was detectable in all tissues. SARS-CoV-2 viral particles were detected byimmunohistochemistry using anti- SARS-CoV-2 nucleocapsid (coat protein) in the lung (positive control), thedistal femoral growth plate, synovium, and femoral epiphysis of infected mice. The SARS-CoV-2nucleocapsid was not detected in the Control lung tissue. Positive cells are stained brown with DABsubstrate, and the sections are counterstained blue with Meyer's Hematoxylin. Scale bars = 50 μ m
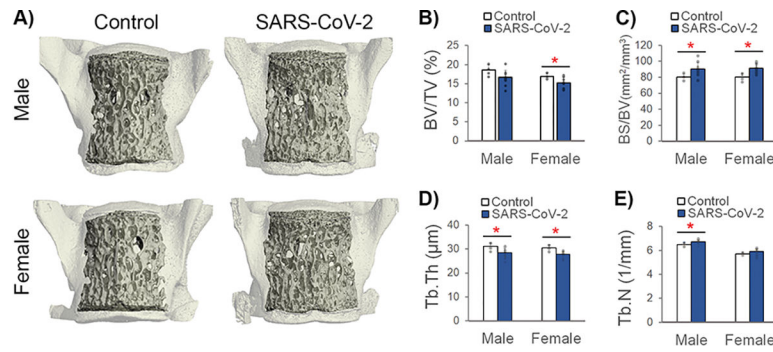
Figure 3.

SARS-CoV-2 induced systemic bone loss in both male and female mice. Representative 3-Drenderings of L5 lumbar spine segments (A). MicroCT showed that SARS-CoV-2 infection was associatedwith a decrease in trabecular bone volume fraction (BV/TV) (B), an increase in specific bone surface (BS/BV)(C), a decrease in trabecular thickness (Tb.Th) (D), and an increase in trabecular number (Tb.N) (E)compared to uninfected Control mice. Significant differences (p<0.05) are indicated by bars with an asterisk(*). MicroCT was performed on SARS-CoV-2 infected mice at 7 ± 2.2 days post-infection (n=24; 12 maleand 12 female) and Control mice at 14 days after mock-inoculation (n=8; 4 male and 4 female).
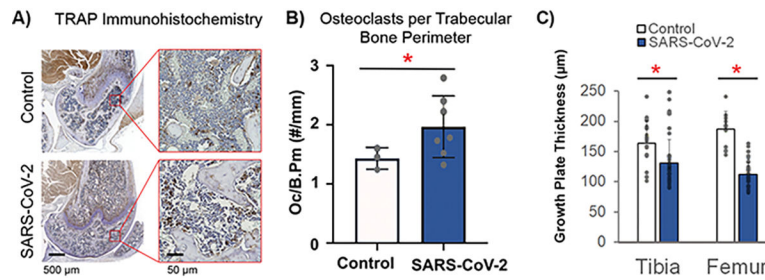
Figure 4.
SARS-CoV-2 infection resulted in increased osteoclast number and decreased growth platethickness. Representative sagittal images of TRAP immunohistochemistry of the femur at day six postinfectionin Control and SARS-CoV-2 infected mice (A). SARS-CoV-2 infection resulted in increased numbersof osteoclasts along the trabecular bone perimeter in the distal femoral epiphysis (n=10 slides: 3 Controlslides and 7 SARS-CoV-2 slides) (B). SARS-CoV-2 infection resulted in decreased growth plate thickness inboth the femur and the tibia by day six post-infection (n=30 slides with 10 measurements per slide: 8Control slides (4 femur and 4 tibia) and 22 SARS-CoV-2 slides (11 femur and 11 tibia) (C). Significantdifferences (p<0.05) are indicated by bars with an asterisk (*).